Progress In Electromagnetics Research C, Vol. 95, 227–238, 2019

Stability Improvement of Analog Adaptive Self-Interference Cancellation System with Phase Compensation

Yunshuo Zhang, Qing Wang*, Huanding Qin, Fangmin He, and Jin Meng

Abstract—The self-interference problem of linear frequency modulated continuous wave (LFMCW) radar is a known issue that limits the radar's detection range. Analog adaptive interference cancellation (AIC) technique is effective to mitigate the self-interference problem. However, we find that the phase difference between the error signal and reference signal paths may significantly deteriorate the stability of the AIC system. Therefore, in this paper, we analyze the effect of phase difference on system stability through the mathematical modeling and simulation. We find that the system is stable when the phase difference is between −90 and 90 degrees, and diverges when it is between 90 and 270 degrees. Therefore, to avoid system instability, we propose to add a phase shifter in the reference signal path to compensate the phase difference. The experiment results show that compared with the traditional delay-based compensation method, our phase compensation based method can increase interference cancellation ratio (ICR) by 15 dB for a single-antenna system and 12 dB for a dual-antenna system.

1. INTRODUCTION

Linear frequency modulated continuous wave (LFMCW) radar is widely used in practice for applications like attitude and range measurements [1]. Since LFMCW radar has to transmit and receive signals at the same time, there is always some leakage of the transmit signal power into the receiver, through antennas or radio frequency (RF) chains. If the self-interference signal power is much higher than echoes signals, the effective measurement range of the LFMCW radar will be limited [2]. Therefore, sufficient isolation between the receiving and transmitting antennas is needed to enable a large measurement range.

At present, there are mainly two types of methods, i.e., passive and active methods, to mitigate the self-interference problem [3]. Passive methods try to avoid the self-interference problem, e.g., by using separate transmit and receive antennas, or by using a duplexer for a single antenna system. Passive methods are effective, but they provide limited isolation, specifically due to limited antenna spacing and duplexer isolation. Instead, active methods, particularly, adaptive interference cancellation (AIC), resort to cancel the interference signal at the receiver. AIC is applicable to both single-antenna and dual-antenna LFMCW radars. In this paper, we focus on the dual-antenna case.

AIC techniques have been applied in LFMCW radars, typically achieving 20–30 dB of self-interference cancellation according to [4–12]. In 2006, Lin et al. proposed a digital AIC system [4]. The system's stability due to the phase difference between feed-through signal and reference signal was compensated by delay lines. However, we find that there may still be a fixed phase error although the time delay is matched. In 2013, Choi and Shirani-Mehr simulated a multi-channel cancellation system. Phase shifters were utilized for Hilbert transformation [5]. The implementation results show that the phase imbalance of phase shifters limits the cancellation performance of this system.

Received 12 July 2019, Accepted 29 August 2019, Scheduled 11 September 2019

* Corresponding author: Qing Wang (qwangwork@163.com).

The authors are with the National Key Laboratory of Science and Technology on Vessel Integrated Power System, Naval University of Engineering, Wuhan, Hubei 430033, China.

The principle of AIC is to generate a cancellation signal that has opposite phase and equal amplitude of the self-interference signal by a vector modulator, and then add the cancellation signal with the self-interference signal to suppress the self-interference [12]. The AIC technique typically employs the Least Mean Square (LMS) algorithm to estimate the amplitude and phase of the cancellation signal, which is realized by a correlator with the reference signal and error signal as inputs. Therefore, reference signal and error signal are required to undergo the same time delay and phase shift [13]. The existing researches, e.g., [4, 12, 14–17], try to match time delay using equal-length transmission lines. However, in actual circuits, especially in analog circuits, some components do not conform to the ideal transmission line model and also introduce fixed phase-shifts. When the phase difference between the circuit paths of the reference signal and error signal is in a certain range, the AIC system will diverge. Therefore, to ensure the stability of the system, we propose to use a phase shifter to compensate the phase difference.

The contributions of this paper are as the follows:

i) We first establish a mathematical model for the AIC system and then analyze the stability condition of the system w.r.t the phase difference of the reference signal and error signal paths.

ii) We propose a system stability improvement method that adds a phase shifter in the reference signal path to compensate the phase difference with respect to the error signal path before input into the correlator. Then, we conduct simulations and experiments to verify the effectiveness of this approach.

The rest of the paper is organized as follows. Section 2 establishes the mathematical model of the AIC system and analyzes the influence of the phase difference on the system. Section 3 presents the experiment results. Conclusion is drawn in Section 4.

2. SYSTEM MODEL

In this section, we establish the mathematical model of an AIC system and then analyze the effect of the phase difference on the system. We will see that the phase difference affects the system stability. When the phase difference is between -90 and 90 degrees, the AIC system is stable and will diverge otherwise. Therefore, it is only necessary to keep the phase shift within the convergence region. We propose to use a phase shifter to compensate the phase difference so as to control the stability of the AIC system. However, it is interesting to find that when the system converges, the value of the phase difference does not affect the interference cancellation ratio (ICR) in steady state.

2.1. AIC System Model

The basic structure of the AIC system is shown in Fig. 1. The Weight Control Circuit is an implementation of the LMS algorithm with analog circuits. Since correlation calculation cannot be done in microwave bands, we first down-convert the microwave-band signals into an intermediate frequency (IF) band, e.g., 280 MHz.

There are several causes of self-interference which may include power leakage between transmitter and receiver antennas and reflections due to nearby objects. However, we usually use antennas that have good directivity. On the one hand, this improves the antenna isolation. On the other hand, this suggests that the signal leakage due to direct coupling is the major source of self-interference. In addition, the coupling channel between the antennas undergoes small channel dispersion, therefore can be treated as a narrow band channel. This assumption is validated by our experimental results that will be presented later.

The reference signal, i.e., the LFM signal can be written as (normalized to have unit power)

$$S_R(t) = e^{-j(2\pi f_c t+\varphi_1)} \tag{1}$$

where $f_c = f_0 + B \cdot t_i/T_M$ is the carrier frequency of the chirped continuous wave; $t_i = t - \lfloor t/T_M \rfloor \cdot T_M$ is the time of the ith sweep period of the LFMCW; $\lfloor . \rfloor$ represents rounding down; B is the sweep bandwidth; T_M is the sweep period; and φ_1 is the phase.

The interference signal, i.e., the signal coupled to the receiver, is

$$S_I(t) = h_0 e^{-j(2\pi f_c t+\varphi_1)} \tag{2}$$

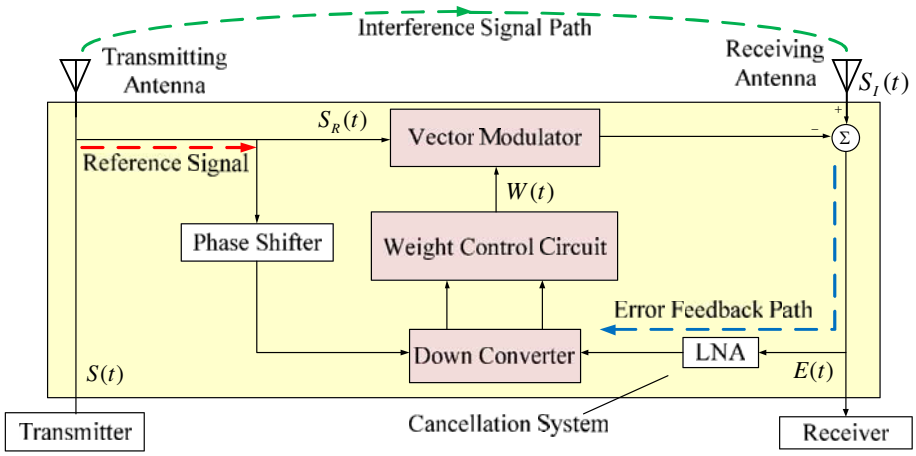

Figure 1. Block diagram of interference AIC system.

where $h_0 = |h_0| e^{-j\theta}$ is the complex coupling channel gain, and θ is the phase difference between the reference signal and interference signal.

The error signal, i.e., the output of the combiner, is obtained as

$$E(t) = S_I(t) - W(t)S_R(t) \tag{3}$$

where $W(t)$ is the weight generated by the weight control circuit which implements the LMS algorithm.

Since the reference signal and error signal pass through different paths to the weight control circuit, they may experience different amplitude and phase changes. Particularly, the error signal path usually consists of a low noise amplifier to increase the error signal power, which is the main factor that produces the phase difference as we have observed from our experiments. Thus the reference signal and error signal input to weight control circuit can be expressed as

$$x(t) = h_R S_R(t) \tag{4}$$

$$e(t) = h_E E(t) \tag{5}$$

where $h_R = |h_R| e^{-j\varphi_R}$, $h_E = |h_E| e^{-j\varphi_E}$ are complex channel gains of the reference signal and error signal paths.

The weight control circuit proposed in this paper is based on LMS algorithm, which uses the reference signal and error signal to calculate the weight control signal. In 1989, Karni and Zeng proposed the steepest descent method for continuous signals to calculate the weight control signal [18], as shown in Eq. (6)

$$\frac{d}{dt}W(t) = \rho e(t)x^*(t) \tag{6}$$

where $\rho > 0$ is the adaptive gain that controls the convergence speed of the LMS filter.

2.2. Convergence Analysis

Substituting Eqs. (4) and (5) into Eq. (6), we can get

$$\frac{d}{dt}W(t) = ue^{j\Delta\varphi}(h_0 - W(t)) \tag{7}$$

where $u = \rho |h_R| |h_E|$, $\Delta\varphi = \varphi_R - \varphi_E$.

Assuming that $W(0) = 1$, the weight signal can be obtained from Eq. (7)

$$W(t) = (1 - h_0)e^{-ue^{j\Delta\varphi}t} + h_0 \tag{8}$$

Substituting Eq. (8) into Eq. (3), we obtain the error signal as

$$E(t) = \sqrt{|h_0|^2 - 2|h_0|\cos\theta + 1} \cdot e^{-ut\cos\Delta\varphi} e^{-j(2\pi f_c t + \varphi_1 + ut\sin\Delta\varphi + \arctan\frac{|h_0|\sin\theta}{|h_0|\cos\theta - 1})} \tag{9}$$

The amplitude of the error signal is

$$|E(t)| = \sqrt{|h_0|^2 - 2|h_0|\cos\theta + 1} \cdot e^{-ut\cos\Delta\varphi} \tag{10}$$

As we can see when time increases, $\lim_{t\to\infty} |E(t)| \to 0$, if $\cos\Delta\varphi \geq 0$. That is, the AIC system is convergent. However, when $\cos\Delta\varphi < 0$, $\lim_{t\to\infty} |E(t)| \to \infty$, the AIC system is divergent.

From the theoretical deduction, we know that the stability of the AIC system is related to the phase difference. When $-90° \leq \Delta\varphi \leq 90°$, the system is stable. However, when $90° < \Delta\varphi < 270°$, the AIC system is divergent. Therefore, in the implementations of the AIC system, the phase difference should be kept within the convergence range. In this paper, a phase shifter is added in the reference signal path to realize the phase compensation.

According to Eq. (9), we conduct the simulation of error signal power over time with different phase differences. Since the isolation between the transceiver antennas used in our experiments is 46 dB, we obtain $|h_0|^2 = 2.26 \times 10^{-4}$. At the same time assume $\theta = \pi/3$, $u = 1$.

The simulation results are shown in Fig. 2. As we can see when phase difference is less than 90 degrees, the AIC system is stable, and the error signal power converges to 0 dBm. Meanwhile, the 90 degrees phase difference is the stable boundary of AIC system, and when it is over 90 degrees the system will be divergent. The above results are consistent with the analysis of the relationship between the phase difference and system stability.

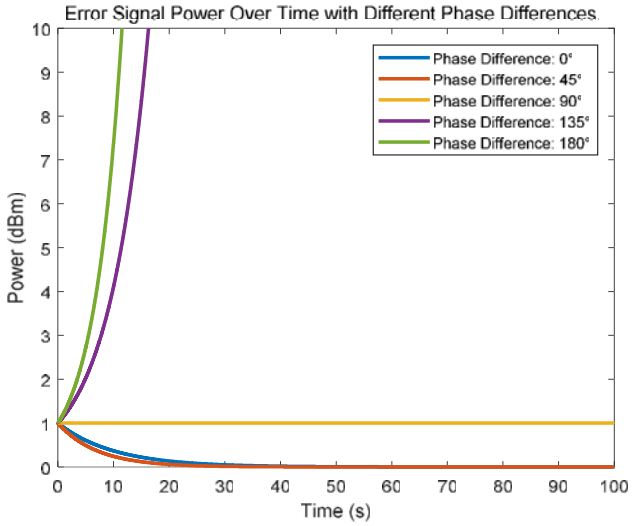

Figure 2. Error signal power over time with different phase differences.

2.3. ICR under Convergence Condition

In this subsection, we provide an analysis of performance of the analog AIC system in the steady state under convergence condition.

The reference signal with noise can be written as

$$S_{RN}(t) = e^{-j(2\pi f_c t + \varphi_1)} + \sigma_n(t) \tag{11}$$

where $\sigma_n(t)$ is the white noise in the reference signal.

According to Eq. (11), the interference signal with noise is obtained as

$$S_{IN}(t) = h_0 e^{-j(2\pi f_c t + \varphi_1)} + \sigma_m(t) \tag{12}$$

where $\sigma_m(t)$ is the white noise in the interference signal. Since the thermal noises are all generated by receivers, it is rational to assume that the white noises have the same power, which can be written as

$$|\sigma_n(t)|^2 = k_n = |\sigma_m(t)|^2 = k_m \tag{13}$$

The error signal obtained by Eqs. (11) and (12) is

$$E_N(t) = S_{IN}(t) - W(t)S_{RN}(t) \tag{14}$$

According [19], we calculate the weight signal by solving the following equation

$$\frac{d}{dt}W(t) = -\rho RW(t) + \rho P \tag{15}$$

where

$$R = E[S_{RN}(t) \cdot S_{RN}^*(t)] \tag{16}$$
$$P = E[S_{IN}(t) \cdot S_{RN}^*(t)] \tag{17}$$

At steady state, we have

$$\frac{d}{dt}W(t) = 0 \tag{18}$$

Then we can obtain weight signal at steady state as

$$\begin{aligned} W(t) &= R^{-1}P = \frac{E(S_{IN}(t) \cdot S_{RN}^*(t))}{E(S_{RN}(t) \cdot S_{RN}^*(t))} \\ &= \frac{h_0}{1+k_n} \end{aligned} \tag{19}$$

Bring Eq. (19) into Eq. (14), then the error signal can be written as

$$E_N(t) = \left(h_0 - \frac{h_0}{1+k_n}\right) e^{-j(2\pi f_c t + \varphi_1)} + \sigma_m(t) - \frac{h_0}{1+k_n}\sigma_n(t) \tag{20}$$

Since the white noise is uncorrelated with other signals, the power of the error signal is the sum of its independent parts [20].

$$\begin{aligned} |E_N(t)|^2 &= \left|h_0 - \frac{h_0}{1+k_n}\right|^2 + \sigma_m^2 - \left|\frac{h_0}{1+k_n}\right|^2 \cdot \sigma_n^2 \\ &= |h_0|^2 \frac{k_n}{1+k_n} + k_m \end{aligned} \tag{21}$$

Then we obtain the ICR model with the noise signal as

$$\begin{aligned} ICR &= 10\log_{10}\frac{|S_{IN}(t)|^2}{|E_N(t)|^2} \\ &= 10\log_{10}\frac{|h_0|^2}{|h_0|^2\frac{k_n}{1+k_n} + k_m} \end{aligned} \tag{22}$$

According to Eq. (22), since $|h_0|^2$ is fixed, the ICR of the AIC system at steady-state depends on noises power. The lower the noise signal power is, the higher the cancellation performance of the AIC system is. However, in actual AIC system the time delay difference, dispersion, and other uncontrollable factors limit the ICR.

To reduce the influence of noise on the cancellation performance, we use passive components, i.e., a coupler to obtain the reference signal, thus k_n can be regarded as 0. Then we obtain ICR model as

$$ICR = 10\log_{10}\frac{|h_0|^2}{k_m} \tag{23}$$

Therefore, the optimum ICR is the SNR of interference signal. We conduct simulation to verify the analysis, and the simulation results are shown in Fig. 3. Under ideal condition, the ICR is equal to the SNR of interference signal.

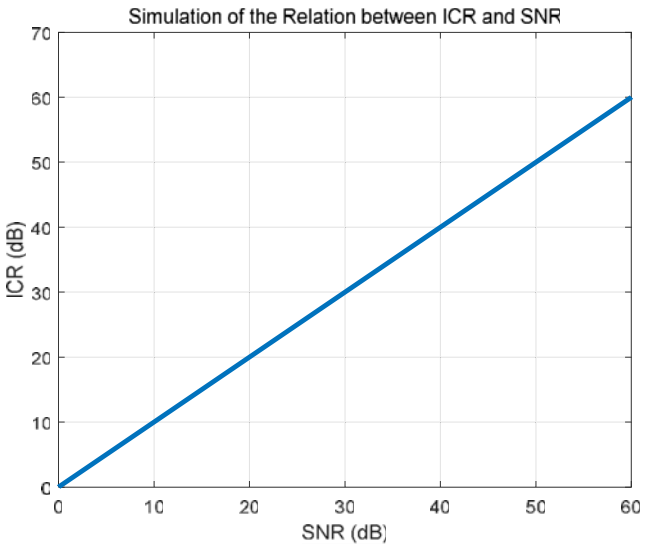

Figure 3. Simulation of the relation between ICR and SNR.

Meanwhile, there is a response time of the LMS algorithm in AIC system, which can be found in [12].

$$t_{loop} = \frac{\Delta\varphi \cdot T_M}{360^\circ \cdot B \cdot \tau} \tag{24}$$

where τ is the time delay. When this response time is large, and the ICR decreases. Practical LFMCW radars usually work in different sweep periods. For a fixed delay and bandwidth, the response time is proportional to the phase difference. Therefore, if the phase difference can be decreased, the cancellation performance will improve.

3. EXPERIMENTAL RESULTS

In this section, we will first analyze the causes of phase difference between the reference signal and error signal path. Then, we provide experimental results to evaluate the ICR performance improvement for a single-antenna system and a dual-antenna system. For the single-antenna system, we utilize an attenuator to replace the duplexer in order to have the same isolation as the dual-antenna case.

3.1. LNA Induced Phase Difference

In an actual AIC system, not all components conform to the transmission line model which states that the phase shift is only determined by the propagation delay [21]. Here, we show an example of the S_{21} characteristics of an LNA with model number ZA60-83LNS+. The test result is shown in Fig. 4. At the center frequency 4.5 GHz, the phase shift when signal passes through LNA is 148.4 degrees, and the time delay is 243.5 ps. According to transmission line assumption, we can calculate the phase shift by $\theta = 2\pi ft$. Theoretical phase shift due to time delay should be 325.6 degrees. Therefore, even though the delays of the reference signal and error signal paths can be calculated to be the same, there is possibly still a phase difference.

3.2. Verification of AIC System Stability Improvement by Phase Compensation

Next, we verify that the phase compensation method is effective in improving the AIC system stability.

In order to evaluate the effect of the phase shifter in the AIC system, we use a variable attenuator to emulate the transmitting and receiving antenna isolation. The experimental parameters are shown in Table 1.

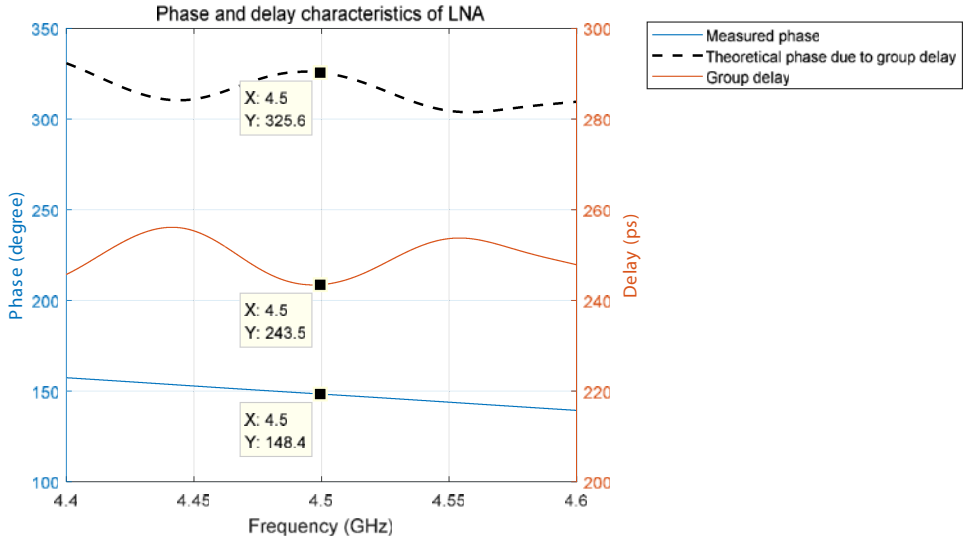

Figure 4. Phase and delay characteristics of LNA.

Table 1. Test parameters.

Center frequency	4.5 GHz
Bandwidth	150 MHz
Signal power	23 dBm
Isolation	46 dB
Sweep Period	100 µs

The results of the experiment compared with theoretical simulation are shown in Fig. 5. Since there is a measurement error of around 30 ps when matching the time delays, the phase difference caused by the measurement error and the LNA is about 89°. Therefore, we shifted the theoretical results by the same degrees.

We can see from Fig. 5 that, when the phase shift is between 0∼179 degrees, the AIC system is stable, however, divergent in 179∼359 degrees. In single-antenna system the maximum ICR is achieved when the phase shift is around 50 degrees, which provides an improvement of 15 dB with respect to 0 degree (i.e., delay matching).

In the dual-antenna system, the ICR reaches 32 dB, and the ICR is improved by about 12 dB. The ICR in dual-antenna system is about 10 dB lower than the single-antenna system because the accuracy of weight signal is affected by the signal reflection in environment and the interference signal dispersion in spatial coupling channel.

In addition, we find that in the single-antenna system when a phase shift is in the range of 50∼100 degrees, the ICR can maintain above 40 dB. For the dual-antenna system, when the phase difference is in the range of 60∼90 degrees, the ICR can maintain above 30 dB. Therefore, the step size of the phase shifter is required to be less than 30 degrees.

The above results show that adding a phase shifter can control the system stability and also improve the performance of the AIC system.

3.3. Single-Antenna System

Based on the study of the effectiveness of using the phase shifter, we further test the AIC system in a single-antenna system setup. According to Section 2.3, the sweep period influences the ICR. Therefore,

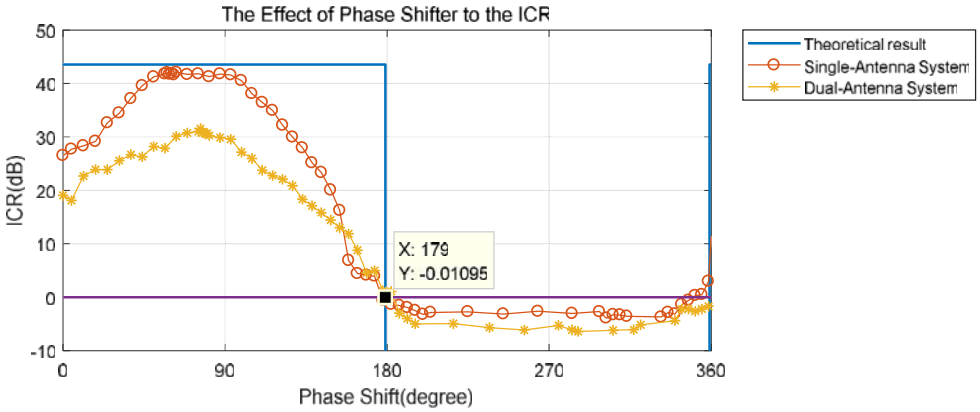

Figure 5. The effect of phase shifter to the ICR.

we also examine the effect of the sweep period in our experiments. The phase shifter is fixed at 62.9 degrees, and the other experiment parameters are the same as Section 3.3.

The experiment results are shown in Fig. 6. Four examples of the interference spectrum before and after cancellation are given in Fig. 7. As we can see, the ICR is around 40∼42 dB, when the phase compensation is on, and in the range of 26∼29 dB when it is off. The phase shifter has improved the ICR by about 15 dB. However, it can be seen that the ICRs in different sweep periods are nearly the same since phase difference is not the only parameter that affects ICR.

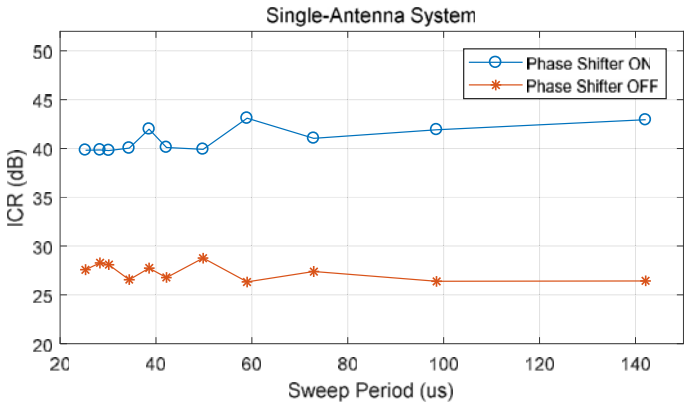

Figure 6. ICR vs sweep period for single-antenna system.

3.4. Dual-Antenna System

In order to estimate the cancellation performance of the AIC system in actual working condition, experiments were conducted using separate transmitting and receiving antennas. Meanwhile, to avoid the indoor reflecting signal entering into the receiving antenna, experiments were carried out in open space field. The dual-antenna system is shown in Fig. 8.

Experiment results are shown in Fig. 9. Four examples of the interference spectrum before and after cancellation are given in Fig. 10. The phase shifter is fixed at 76.4°. The other experiment parameters are the same as the single-antenna system. It can be seen that when the phase shifter is on, the ICR is in the range of 30∼32 dB, which is lower than the single-antenna experiments. When the phase shifter is off, the ICR is in the range of 16.5∼20 dB. In dual-antenna system, the phase shifter has improved the ICR by about 12 dB. Again, the sweep period does not affect the ICR.

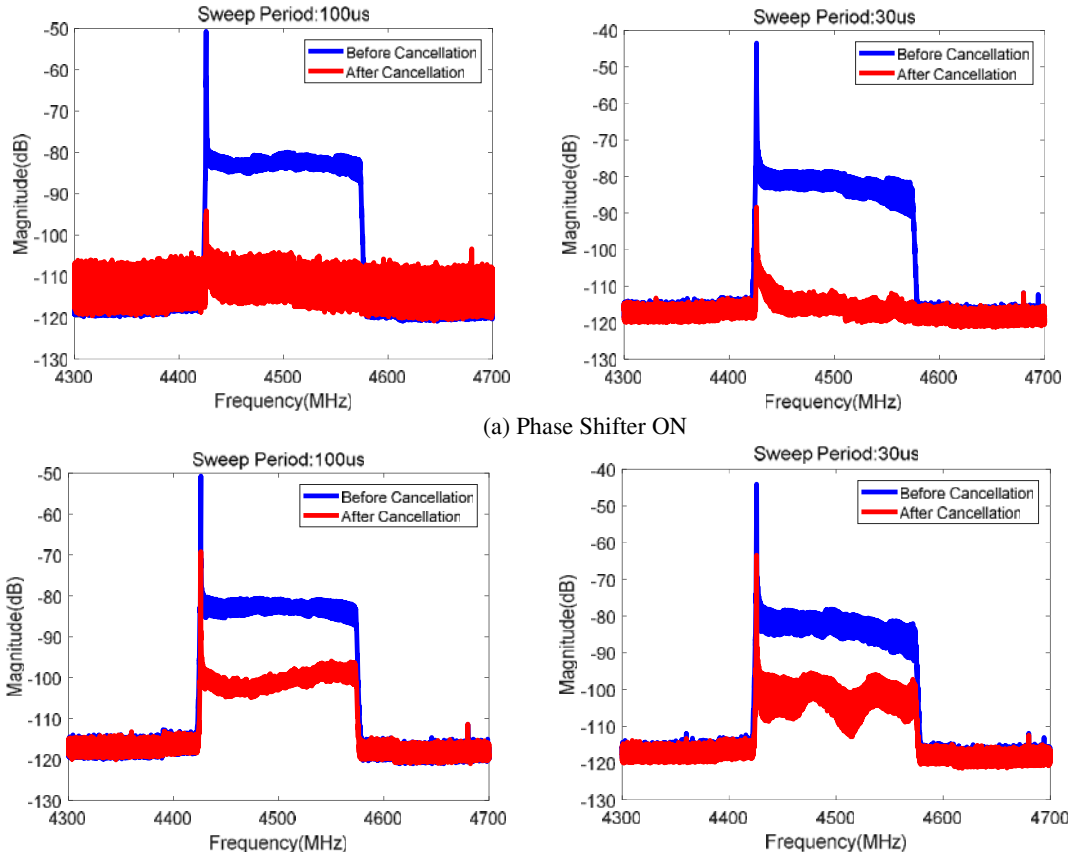

(a) Phase Shifter ON

(b) Phase Shifter OFF

Figure 7. Spectrum of the error signal before and after cancellation.

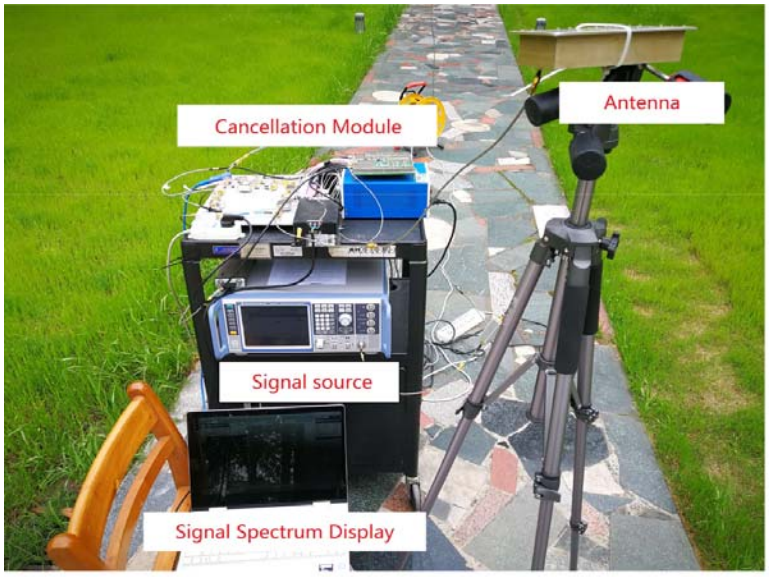

Figure 8. Dual-antenna experiment system.

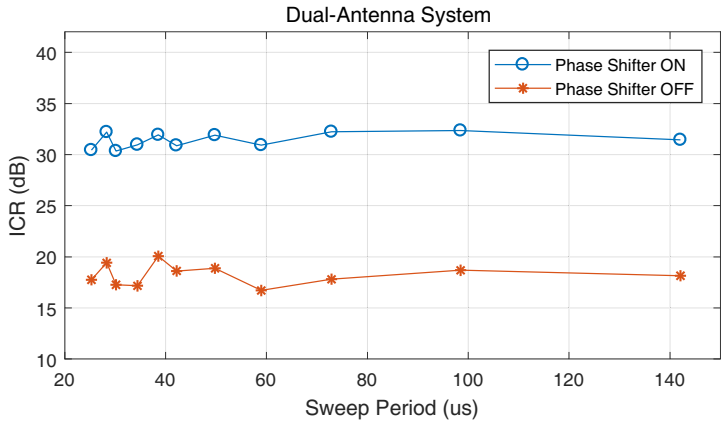

Figure 9. ICR vs sweep period for dual-antenna system.

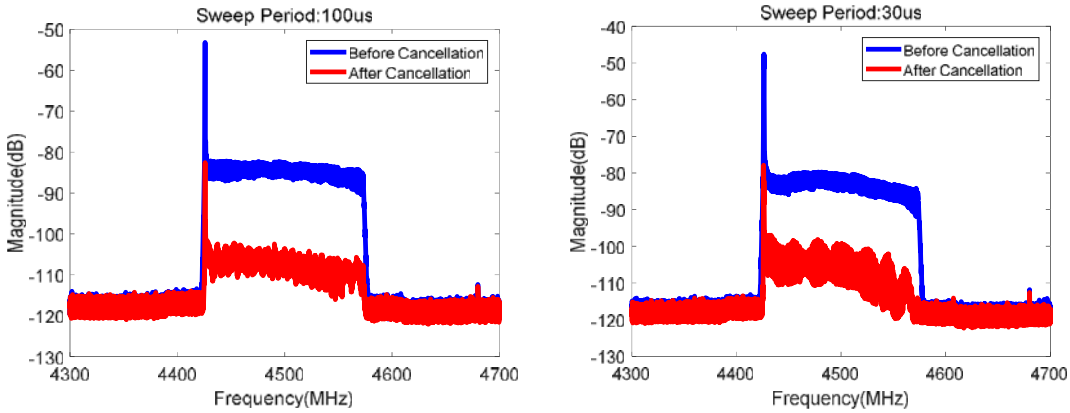

(a) Phase Shifter ON

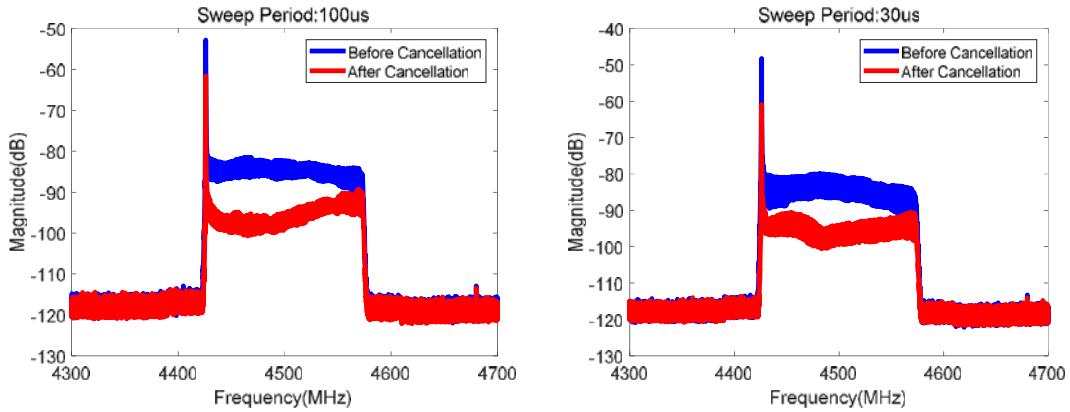

(b) Phase Shifter OFF

Figure 10. Spectrum of the error signal before and after cancellation.

4. CONCLUSIONS

In this paper, we have analyzed the effect of the phase difference of the error signal and reference signal paths on the behavior of analog AIC system. We have found that when the phase difference is between 90 and 270 degrees, the AIC system will diverge. Therefore, we propose to add a phase shifter in the reference signal path to compensate the phase difference. The proposed technique is then implemented to test its effectiveness. Experiment results show that phase compensation can improve the AIC system

stability as our theory has suggested. In addition, it is interesting to find that phase compensation can also improve the ICR in actual systems. The maximum ICR improvement that we have observed is around 15 dB. Using the proposed phase compensation method, our analog AIC system offers an ICR of 42 dB in a single-antenna system, which is significantly better than the ones reported in the literature. When experimenting with a dual-antenna system, the ICR for a signal as large as 150 MHz can also be as high as 32 dB. These results verify the effectiveness of the proposed phase compensation method.

REFERENCES

1. Quiroz, A. E. N. and W. Josef, "Towards a full-duplex CW radar: Development of a reflected power canceller in digital domain," *ACM International Conference Proceeding Series*, 21–26, Nov. 2017.
2. Wang, Q., F. He, H. Liu, K. Zhao, and J. Meng, "Adaptive spatial filtering for interference cancellation between Co-site phased arrays," *IEEE 2018 Asia-Pacific International Symposium on Electromagnetic Compatibility (APEMC)*, 451–455, Jun. 2018.
3. Nawaz, H., Ö. Gürbüz, and I. Tekin, "High isolation slot coupled antenna with integrated tunable self-interference cancellation circuitry," *Electronics Letters*, Vol. 54, No. 23, 1311–1312, Nov. 2018.
4. Lin, K., Y. E. Wang, C. K. Pao, and Y. C. Shih, "A Ka-band FMCW radar front-end with adaptive leakage cancellation," *IEEE Transactions on Microwave Theory & Techniques*, Vol. 54, No. 12, 4041–4048, Dec. 2006.
5. Choi, Y. S. and H. Shirani-Mehr, "Simultaneous transmission and reception: Algorithm, design and system level performance," *IEEE Transactions on Wireless Communications*, Vol. 12, No. 12, 5992–6010, Dec. 2013.
6. Kim, S., Y. Jeon, G. Noh, Y. O. Park, L. Kim, and H. Shin, "A 2.59-GHz RF self-interference cancellation circuit with wide dynamic range for in-band full-duplex radio," *2016 IEEE MTT-S International Microwave Symposium (IMS)*, 1402–1405, Aug. 2016.
7. Lu, H., C. Huang, M. Tarantez, S. Schwarz, and S. Shao, "Quadrature down-conversion based analog self-interference cancellation for continuous wave radars," *2016 IEEE Globecom Workshops (GC Wkshps)*, 1–6, Feb. 2017.
8. Ponnekanti, S. and S. Sali, "Non-linear interference cancellation techniques for electromagnetically dense propagation environments," *Progress In Electromagnetics Research*, Vol. 18, No. 5, 209–228, Jan. 1998.
9. Orimoto, H. and A. Ikuta, "Signal processing for noise cancellation in actual electromagnetic environment," *Progress In Electromagnetics Research*, Vol. 99, 307–322, Jan. 2009.
10. Jiang, Y., W. Ma, and Z. Zhao, "Influence of non quadrature of phase shifter to adaptive interference cancellation system," *2009 International Conference on Intelligent Human-Machine Systems and Cybernetics*, 1–5, Nov. 2009.
11. Huang, X. and Y. J Guo, "Radio frequency self-interference cancellation with analog least mean-square loop," *IEEE Transactions on Microwave Theory and Techniques*, Vol. 65, No. 9, 3336–3350, Feb. 2017.
12. Beasley, P. L. D., A. G. Stove, B. J. Reits, and B. As, "Solving the problems of a single antenna frequency modulated CW radar," *IEEE International Radar Conference*, 391–395, 1990.
13. Qin, H., J. Meng, F. He, and Q. Wang, "A microwave interference cancellation system based on down-conversion adaptive control," *IEEE International Conference on Communication Technology*, 364–368, Jan. 2019.
14. Li, W., J. Meng, J. Tang, F. He, and L. Yi, "Interference cancellation system instantaneous bandwidth and time delay problem research," *2016 Asia-Pacific International Symposium on Electromagnetic Compatibility (APEMC)*, 1–3, Jul. 2016.
15. Chang, M. P., C. L. Lee, B. Wu, and P. R. Prucnal, "Adaptive optical self-interference cancellation using a semiconductor optical amplifier," *IEEE Photonics Technology Letters*, Vol. 27, No. 9, 1018–1021, Feb. 2015.

16. Sun, J. J., M. P. Chang, and P. R. Prucnal, "Demonstration of over-the-air RF self-interference cancellation using an optical system," *IEEE Photonics Technology Letters*, Vol. 29, No. 4, 397–400, Jan. 2017.
17. Le, A. T., L. C. Tran, X. Huang, Y. J. Guo, and J. Y. C. Vardaxoglou, "Frequency-domain characterization and performance bounds of ALMS loop for RF self-interference cancellation," *IEEE Transactions on Communications*, Vol. 67, No. 1, 682–692, Aug. 2018.
18. Karin, S. and G. Zeng, "The analysis of the continuous-time LMS algorithm," *IEEE Transactions on Acoustics, Speech, and Signal Processing*, Vol. 37, No. 4, 595–597, Apr. 1989
19. Haykin, S., *Adaptive Filter Theory*, 5th Edition, 2014.
20. Oppenheim, A. V., *Signals & Systems*, 2nd Edition, 2013.
21. Xiao, H., Z. Zhao, J. Tang, Y. Li, W. Li, and C. Luo, "The influence of time delay between interference signal and reference signal to the interference cancellation system," *2011 4th IEEE International Symposium on Microwave, Antenna, Propagation and EMC Technologies for Wireless Communications*, 1–4, Feb. 2012.